

Optical evidence for the spin-state disorder in $\text{LaCo}_{1-x}\text{Rh}_x\text{O}_3$

Ichiro Terasaki, Shinichiro Asai, Hiroki Taniguchi

Department of Physics, Nagoya University, Nagoya 464-8602, Japan

Ryuji Okazaki

Department of Physics, Faculty of Science and Technology, Tokyo University of Science,
Noda 278-8510, Japan

Yukio Yasui

Department of Physics, Meiji University, Kawasaki 214-8571, Japan

Yuka Ikemoto, Taro Moriwaki

Japan Synchrotron Radiation Research Institute (JASRI), SPring-8, Sayo, Hyogo 679-5198,
Japan

Abstract. We have measured the infrared reflectivity of single-crystalline samples of $\text{LaCo}_{1-x}\text{Rh}_x\text{O}_3$ ($x = 0, 0.05$ and 0.10) from 10 to 300 K from 0.05 to 0.15 eV. We find that the optical phonons of the Co-O stretching mode depend on temperature and the Rh content. Analysis with three Lorentz oscillators reveals that the spin state of Co^{3+} in $\text{LaCo}_{1-x}\text{Rh}_x\text{O}_3$ can be understood in terms of a solid solution of low-spin- and high-spin-state Co^{3+} ions, and the substituted Rh ion retains some fraction of the high-spin Co^{3+} ions down to low temperature.

1. Introduction

The spin state is a fundamental concept in the transition-metal complexes and compounds, [1, 2] where the Hund coupling between d electrons competes with the electric potential formed by the surrounding anions called “ligand field”. When the Hund coupling is dominant, the total spin of d electrons on the transition-metal ion is maximized. In contrast, when the ligand field effect is strong, the d electrons occupy the low-lying energy levels first. The former is called “the high-spin state”, and the latter “the low-spin state”.

An important case is the trivalent cobalt ion.[3] In this particular ion, the six d electrons can take either the high spin state of $t_{2g}^4 e_g^2$ with a total spin of $S = 2$ or the low spin state of t_{2g}^6 with $S = 0$, when the Co^{3+} ion is surrounded with six octahedrally-coordinated anions. The two states are almost degenerate in energy, and the spin state can change with temperature,[3, 4, 5] pressure,[6, 7] structure,[8] and magnetic field.[9] In addition, an intermediate spin state has been proposed theoretically,[10] and there has been a hot debate on the existence of this spin state in LaCoO_3 . [11, 12, 13, 14, 15]

We have studied the spin-state control in Co and Rh oxides, [16, 17, 18, 19] and have found that partial substitution of Rh for Co induces weak ferromagnetism in LaCoO_3 . [20, 21, 22, 23] In LaCoO_3 , all the Co^{3+} ions start to fall into the low spin state below around 100 K, and show the non-magnetic ground state, being known as spin-state crossover.[24] We found that the Rh substituted samples remain magnetic down to 2 K, and claim that the Rh substitution suppresses the spin-state crossover. Assuming that the thermodynamic quantities of $\text{LaCo}_{1-x}\text{Rh}_x\text{O}_3$ can be understood in terms of a solid solution of Co^{3+} ions of different spin states, we proposed that the substituted Rh ion lets some of the neighboring Co^{3+} ions be in the high-spin state down to lowest temperatures measured. This proposal explains the Rh content dependence of the magnetism [20] and lattice volume.[22] This is supported by an ab-initio calculation, where the substituted Rh ion with a large size increases elastic energy to let a Co ion in a next nearest neighbor site be in the high-spin state.[25] In addition, we found that the Ga substitution accelerates the spin-state crossover,[21] and showed the solid solution model for the spin states also explains the experiments well. In the course of these studies, we have proposed that the spin states of LaCoO_3 are better understood as a mixture of low and high spin states rather than intermediate spin state.

We have measured and analyzed the thermodynamic quantities with the spin-state mixture model. Since these quantities were obtained from the volume average, microscopic evidence for the spin-state mixture is necessary to consolidate our idea. Here we show the optical evidence for the spin-state mixture in $\text{LaCo}_{1-x}\text{Rh}_x\text{O}_3$. Optical phonons are a good probe for the microscopic information on the spin state through the different ionic sizes. In addition, they are less surface sensitive compared with photoemission experiments, and give reliable information on bulk properties. We have observed that the spin states are highly disordered in the optical spectra of the Rh-substituted samples, and have found that the disorder in the optical phonons is consistent with our idea of the spin-state mixture in LaCoO_3 .

2. Experimental

Single crystals of $\text{LaCo}_{1-x}\text{Rh}_x\text{O}_3$ ($x = 0, 0.05, 0.10$) were grown by a floating zone method from polycrystalline rods of $\text{LaCo}_{1-x}\text{Rh}_x\text{O}_3$ in an infrared-heating furnace (Crystalsystems, FZ-F4000-H-I-V). The polycrystalline rods were prepared by a conventional solid-state reaction method. A mixture of La_2O_3 (99.9%), Co_3O_4 (99.9%), and Rh_2O_3 (99.9%) with stoichiometric molar ratio was ground, and calcined for 24 h at 1000°C in air. The calcined powder was ground, pressed into a 70-mm long rod with a 6-mm radius, and sintered for 48 h at 1200°C in air. A single crystal of LaCoO_3 was used as a seed rod in order to trigger crystal growth. The size of the obtained single crystal is a 10-mm long rod with a 4-mm radius.

The sample was characterized by x-ray diffraction with a standard Laue camera (Rigaku 4037V), and was found to be of multiple domains (mosaic crystal). The domain size seemed to decrease with the Rh content x . Magnetization was measured in a field cooling process of 1 T using a superconducting quantum interference device magnetometer (Quantum Design MPMS).

Since a mechanically polished surface may give extrinsic spectrum in a strong electron-phonon coupled materials, as-cleaved surfaces with a typical dimension of $1 \times 0.5 \text{ mm}^2$ were used for the infrared measurement. Since the multiple-domain samples did not have cleavage planes, the cleaved surface was rugged. In order to compensate the roughness of the surface, a gold film was evaporated at the half of the cleaved surface, and used as a reference. The polarized reflectivity spectra in a area of $30 \times 30 \mu\text{m}^2$ on the crystal surface were measured for energies between 0.05 and 0.15 eV using a Fourier transform infrared spectrometer equipped with an infrared microscope at the Beam Line 43IR, SPring-8, Japan.[26] The reflectivity mapping was performed, but no significant spacial dependence was observed in the whole surface of the samples. Owing to the rough surface, the magnitude of the reflectivity was randomly scattered from plane to plane from temperature to temperature, and we normalized the reflectivity around 0.15 eV to coincide with the value for $x = 0$ at 300 K. The samples were set in an optical cryostat (Oxford Microstat) and were cooled with helium gas flow. The temperatures were monitored at the sample mount of copper metal by a resistance thermometer.

3. Results and Discussion

Figure 1 shows the optical reflectivity spectra of $\text{LaCo}_{1-x}\text{Rh}_x\text{O}_3$ single crystals. The spectra for $x = 0$ shown in Fig. 1(a) exhibit one broad peak around 0.07-0.08 eV at 10 K, which is assigned to the stretching mode of Co and O in the CoO_6 octahedra. With increasing temperature, the peak splits into two sharper peaks, and the lower energy peak around 0.07 eV seems to lose intensity with temperature. These features are consistent with the previous measurements, [27] and the two reflectivity peaks have been assigned to the Co–O stretching mode of the different spin states.[28]

The Rh substituted samples show room-temperature reflectivity spectra roughly identical to $x = 0$ except for poor signal-to-noise ratios coming from the rough surface. In contrast, the

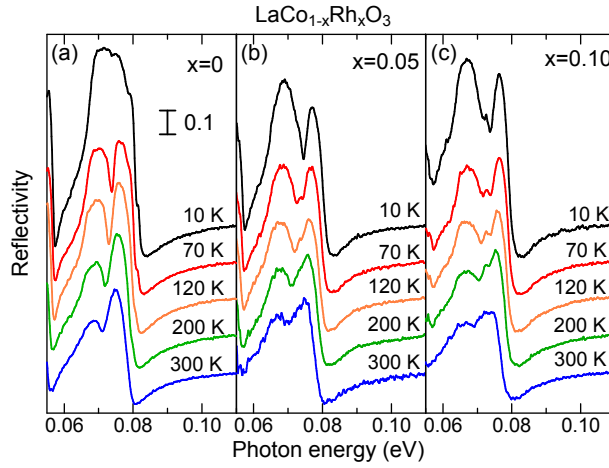


Figure 1. (Color online) Reflectivity spectra of $\text{LaCo}_{1-x}\text{Rh}_x\text{O}_3$ single crystals. (a) $x = 0$, (b) $x = 0.05$ and (c) $x = 0.10$. The zero point of the reflectivity spectra are properly shifted to see each spectrum clearly.

low-temperature spectra show a remarkable difference from $x = 0$; They show the two-peak structure even at 10 K, and the spin states at room temperature seem to hold down to 10 K. This is consistent with our previous observation of the spin-state crossover suppression by the Rh substitution.[20] By carefully looking at the spectra, one may find an additional small peak between the large peaks around 0.73 eV for $x = 0.10$.

Owing to the limited energy range, the Kramers-Kronig analysis may give less reliable information in the present experiment. Instead we fit the reflectivity data with three Lorentz oscillators given by

$$\frac{\varepsilon}{\varepsilon_0} = \varepsilon_\infty + \sum_{i=1}^3 \frac{C_i}{\omega_i^2 - \omega^2 - i\omega\gamma_i}, \quad (1)$$

where C_i , ω_i and γ_i are the oscillator strength, the resonance frequency and the damping factor of the i -th oscillator, respectively. The high-frequency dielectric constant ε_∞ was set to be 6.75.

The reflectivity R for normal incidence light is a complicated function of the complex refractive index $\tilde{n} = n - ik$ expressed by

$$R = \frac{(n-1)^2 + \kappa^2}{(n+1)^2 + \kappa^2}. \quad (2)$$

The complex dielectric constant $\tilde{\varepsilon} = \varepsilon_1 - i\varepsilon_2$ is also expressed by \tilde{n} as

$$\varepsilon_1/\varepsilon_0 = n^2 - \kappa^2 \quad (3)$$

$$\varepsilon_2/\varepsilon_0 = 2n\kappa, \quad (4)$$

or inversely, n and κ are expressed in terms of $\tilde{\varepsilon}$ as

$$n = \sqrt{\frac{\varepsilon_1 + \sqrt{\varepsilon_1^2 + \varepsilon_2^2}}{2\varepsilon_0}} \quad (5)$$

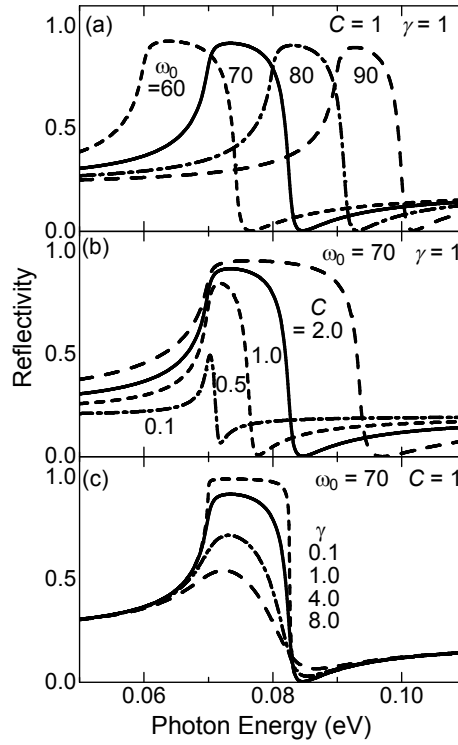


Figure 2. Reflectivity calculated with one Lorentz oscillator. ω_0 is the resonance frequency in meV unit, and γ is the damping factor in meV unit. The oscillator strength C is properly normalized value.

$$\kappa = \sqrt{\frac{-\varepsilon_1 + \sqrt{\varepsilon_1^2 + \varepsilon_2^2}}{2\varepsilon_0}}. \quad (6)$$

Accordingly, even if the dielectric function is given by a simple summation of three Lorentz oscillators, the reflectivity depends on each parameter in a complicated way.

In order to see how the parameters of the Lorentz oscillator affect the reflectivity, we have calculated reflectivity spectra for a single Lorentz oscillator

$$\frac{\varepsilon}{\varepsilon_0} = \frac{C}{\omega_0^2 - \omega^2 - i\omega\gamma} + \varepsilon_\infty (= 6.75) \quad (7)$$

in Fig. 2. Figure 2 (a) shows the ω_0 dependence for fixed values $C = 1$ and $\gamma = 1$ meV. The value of ω_0 determines the photon energy above which the reflectivity sharply increases. Figure 2(b) shows the C dependence for fixed values of $\omega_0 = 70$ meV and $\gamma = 1$ meV. The value of C determines the photon energy at which the reflectivity has an edge. Simultaneously, as the reflectivity edge comes close to ω_0 , the shape of the reflectivity changes from a square to a peak around ω_0 . Figure 2 (c) shows the γ dependence for fixed values of $\omega_0 = 70$ meV and $C = 1$. The value of γ determines the sharpness of the square-shape spectra.

By comparing Fig. 2 with the spectrum for $x = 0$ at 10 K in Fig. 1, one may notice that a single Lorentz oscillator can fit the observed spectra fairly well, and the sharpness of the reflectivity rise near 0.07 eV and the reflectivity edge near 0.08 eV implies a small value of γ . Figure 3 shows typical examples for the fitting. For the spectrum of $x = 0$ at 10 K,

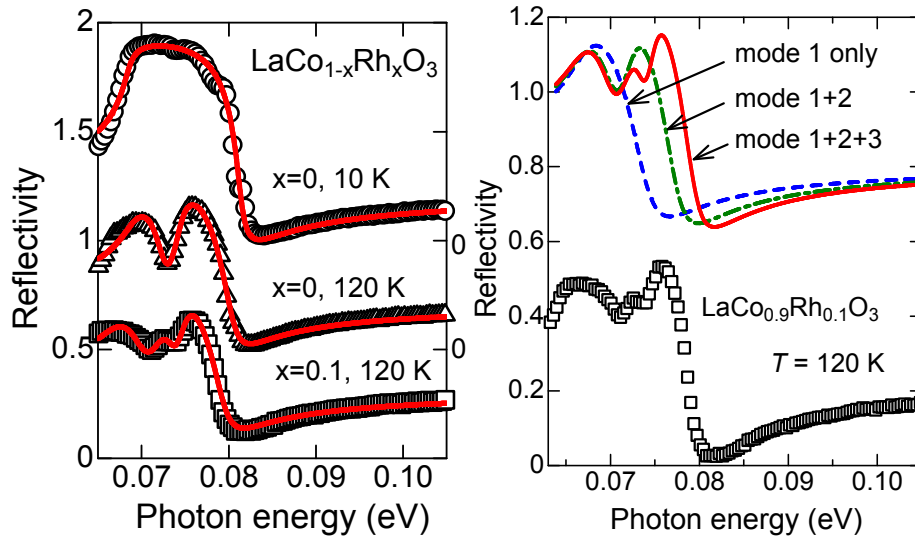


Figure 3. (Color online) Left panel: Comparison of the measured data and with the fitting with three Lorentz oscillators. The open symbols denote the measurement data, and the solid curves represent the fitting results. The top curve ($x = 0$ at 10 K) is fit with one Lorentz oscillator, the middle ($x = 0$ at 120 K) fit with two oscillators, and the bottom ($x = 0.1$ at 120 K) is fit with three oscillators. The three spectra are plotted by shifting the zeros by 0.5, as indicated at the right axis. Right panel: the contributions of the three Lorentz oscillators to the reflectivity spectrum shown by fitting curves with one, two and three oscillators. The calculated curves are vertically shifted by 0.6.

only one oscillator can fit the spectrum satisfactorily. We tried to fit the spectra with two oscillators, and found that C_2 is negligibly small. In contrast, the two oscillators fit well for $x = 0$ at higher temperatures, as shown in the middle figure of Fig. 3. As mentioned above, the small peak appears between the two large peaks in the Rh-substituted sample, and the spectra for $x = 0.05$ and 0.10 are fit with three Lorentz oscillators, as shown in the bottom figure of Fig. 3. In the right panel of Fig. 3, we show how the three oscillators affect the shape of the reflectivity. As is clearly seen, the two Lorentz oscillators (mode 1 +2) explain the gross feature of the reflectivity. In order to fit the three peak structure, we have added one more oscillator (mode 1+2+3). By doing so, the peak of the mode 2 becomes smaller by interfering with the mode 3 even if all the parameters for the mode 2 remain the same. This clearly indicates complicated dependence of the fitting parameters.

Figures 4(a)–(c) show the resonance frequencies obtained through fitting with Eq. (1). The lowest frequency ω_1 shows a slight red-shift below 100 K, and decreases with increasing Rh content x . ω_2 also decreases with x slightly, and shows temperature dependence weaker than ω_1 . ω_3 is almost independent of temperature and the Rh content.

Figures 4(d)–(f) show the damping factors. All the damping factors decrease with decreasing temperature, suggesting that the inelastic scattering decreases with decreasing thermal energy $k_B T$. By taking a closer look at the magnitudes, one may find that γ_1 for $x = 0$ is smallest, and reaches 1.5 meV at 10 K. Although this value is of the same order of $k_B T$, the phonon excitation can be long-lived in LaCoO_3 at low temperatures. This is reasonable

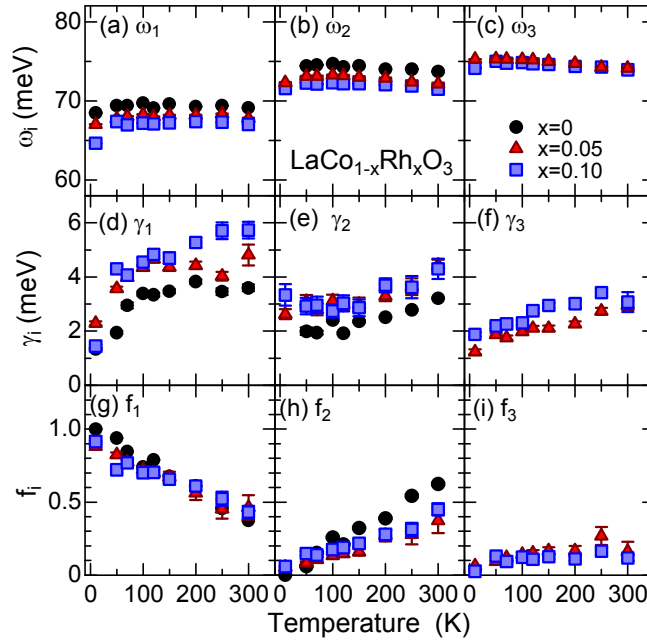


Figure 4. (Color online) The parameters obtained by fitting the measured reflectivity spectra, being plotted as a function of temperature for $x = 0, 0.05$ and 0.10 . (a)–(c) The resonance frequencies, and (d)–(f) the damping factors. (g)–(i) The normalized oscillator strength f_i . Since the total strength changes with temperature, each oscillator strength C_i is normalized by the total strength of $C_1 + C_2 + C_3$ at each temperature given as $f_i(T) = C_i(T) / \sum_j C_j(T)$.

because all the Co^{3+} ions are in the low spin state at low temperature. The lattice vibration can be harmonic because all the Co ions have a single ion size. In contrast, γ_1 and γ_2 for $x = 0.05$ and 0.10 are significantly larger than $k_B T$ at 10 K, and almost independent of x . This means that the optical phonons related to magnetic Co^{3+} ions are severely disordered, in which the 10% static disorder by Rh is negligible. We should note that the obtained values of ω_1 , γ_1 , ω_2 and γ_2 for $x = 0$ are consistent with the previous work [28], where the phonon spectra are plotted using the imaginary part of the dielectric constant ϵ_2 . In Ref. [28], the reflectivity data were converted into the dielectric constant through the Kramers-Kronig relation, and the raw data of the reflectivity spectra were not shown.

Now let us attribute the three Lorentz oscillator to the different spin states. Before doing so, we should remind ourselves that phonons are collective excitations of the lattice motion in question, and cannot be assigned to a single local atom as one-to-one correspondence, in general. For example, optical and acoustic modes are defined in a binary lattice consisting of atom A and B, but it makes little sense which mode is assigned to atom A.

Nonetheless, we can associate the three phonons with different ions in the different spin states in the present case. As mentioned above, the three phonon modes are highly disordered, and the disorder is dynamical in the sense that the static disorder by the 10% Rh substitution plays a secondary role. Considering that each Co ion finds more than one Rh ion within the next nearest neighbor sites for the $x = 0.10$ sample, we suggest that the length scale of the static and dynamical disorder is of the order of unit cell. In such a situation, we cannot

expect collective motion of the lattice vibration, and all the optical phonon modes are well localized. Actually, according to a recent inelastic x-ray scattering experiment,[29] the optical phonons are almost dispersionless in LaCoO_3 , and different phonon modes have been assigned to different spin states.

Considering the above situations, we will assign the three phonon modes. The ω_1 mode corresponds to the Co ions in the low spin state, because this mode is the one observed in $x = 0$ at 10 K. Likewise, the ω_2 mode corresponds to the Co ions in the high-spin state, because all the parameters of ω_2 , γ_2 and f_2 show similar temperature dependence among the $x = 0, 0.05$ and 0.10 samples.

The assignment of the ω_3 mode includes some uncertainty. This mode appears only for $x > 0$, and thus it should be naturally assigned to the Rh ion. However, as the ab-initio calculation reveals,[25] the substituted Rh ion can statically induce a high-spin-state Co ion at a next nearest neighbor site. The two positionally-correlated ions have a similarly large ion size, and are difficult to distinguish from the lattice vibration. Thus we assign the ω_3 mode to the Rh ion *and* the high-spin-state Co^{3+} ion statically induced by Rh. According to our assignment, the phonon mode for the low spin state is 65–70 meV, being lower than that for the high-spin state of 70–75 meV. This can be understood by considering the larger ion size of the high-spin-state Co^{3+} , which is also suggested from a first-principle calculation.[30]

Assuming that the stretching-mode phonons are well localized, we can associate the oscillator strength with the fraction of the Co ions in the different spin-states. Figures 4(g)–(i) show the normalized oscillator strength f_i given by $f_i(T) = C_i(T) / \sum_j C_j(T)$. We find that the total strength of $C_1 + C_2 + C_3$ linearly increases with decreasing temperature from 300 down to 10 K. The origin for this temperature dependence is yet to be explored, but we notice that the electronic contribution is not included in the fitting. $\text{LaCo}_{1-x}\text{Rh}_x\text{O}_3$ are non-metallic, and there should be a significant contribution of Drude-like excitation at high temperatures, which may screen the optical phonon excitations. The Kramers-Kronig analysis could separate these excitations, if the experiment were extended to a wider energy range. Increase in f_1 and decrease in f_2 simultaneously happen. We notice that f_3 is not proportional to x , which looks incompatible with our assignment. This mode corresponds to a pair of a Rh ion and the induced high-spin-state Co ion. In $x = 0.10$, the pairs partially overlap, in which the relationship of $f_3 \propto x$ is no longer valid. However, we cannot deny that this may be simply due to uncertainty of the fitting of three Lorentz oscillators.

Let us compare the analysis of the Lorentz oscillators with the magnetism of the title compound. Figure 5(a) shows the product of the magnetization M and temperature T in $\text{LaCo}_{1-x}\text{Rh}_x\text{O}_3$. Here we assume an oversimplified picture that the high-spin state of Co^{3+} ions distribute randomly and homogeneously in the samples, and act as independent magnetic impurities at sufficiently low temperature. On this picture, the susceptibility χ follows the Curie law of $\chi = C/T$, and the density of the magnetic moment is proportional to χT . In the present case, the ground state of $x = 0.05$ and $x = 0.10$ is weak ferromagnetic, and we use MT instead of χT for the analysis. As shown in Fig. 5(a), the MT values decrease with decreasing temperature from 300 K indicating that the magnetic moments (high-spin state Co^{3+}) decrease with decreasing temperature. For $x = 0$, the value is almost zero at 4 K,

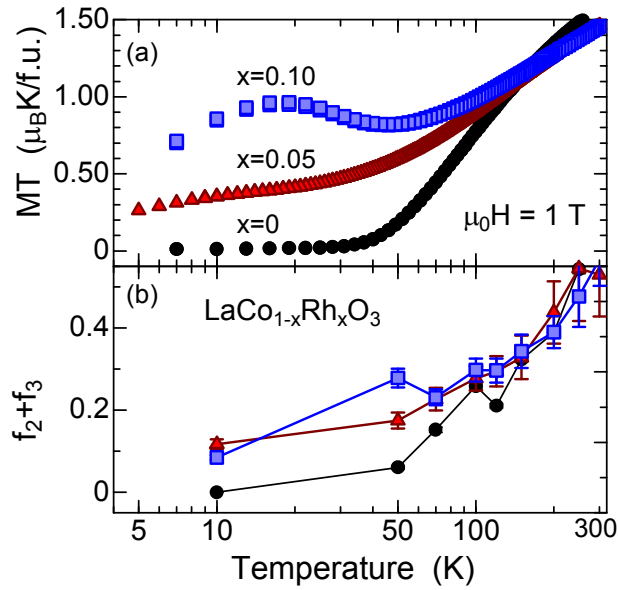


Figure 5. (Color online) (a) The product of magnetization M and temperature T and (b) The fraction of magnetic ions $1 - f_1 = f_2 + f_3$ in $\text{LaCo}_{1-x}\text{Rh}_x\text{O}_3$ plotted as a function of temperature.

showing the nonmagnetic ground state. For $x > 0$, the MT values remain finite at 4 K, which are responsible for the weak ferromagnetism.

Figure 5(b) plots the magnetic-ion contribution in the Lorentz oscillators. Since we assigned f_1 to the low-spin-state contribution, we plot $1 - f_1 = f_2 + f_3$ as a function of temperature. All the data decreases with decreasing temperature, and the data for $x > 0$ remain finite at 10 K. Also one may notice that the gross features look similar between MT and $f_2 + f_3$. This supports that the magnetic states in $\text{LaCo}_{1-x}\text{Rh}_x\text{O}_3$ we proposed from thermodynamic measurements are quantitatively consistent with the optical spectroscopy—a microscopic probe for bulk properties.

4. Summary

We have measured and analyzed the infrared reflectivity spectra of $\text{LaCo}_{1-x}\text{Rh}_x\text{O}_3$ ($x = 0, 0.05$ and 0.10). The room-temperature spectra are almost independent of x , and the phonon modes are dynamically disordered even for $x = 0$. The analysis using three Lorentz oscillators has revealed that the room temperature spectra are well understood in terms of a mixture of localized phonon modes of the Co^{3+} ions in the low and high spin states. The Rh substituted samples essentially hold the features of the room-temperature spectra of $x = 0$ down to 10 K, which is consistent with the suppression of the spin-state crossover in the Rh-substituted LaCoO_3 . The present work is a piece of microscopic evidence of the spin state disorder in LaCoO_3 , and consolidates our proposal that the physical properties of LaCoO_3 can be understood in terms of a mixture of Co ions in the high and low spin states.

This work was partially supported by the Program for Leading Graduate Schools, Japan Society for the Promotion of Science. The synchrotron radiation experiments were performed

at the BL43IR of SPring-8 with the approval of the Japan Synchrotron Radiation Research Institute (JASRI) (Proposal No. 2012B1674).

References

- [1] S. Sugano, Y. Tanabe, and H. Kamimura. *Multiplets of transition-metal ions in crystals*. Academic Press, New York, 1970.
- [2] Philipp Gülich, Yann Garcia, and Harold A. Goodwin. Spin crossover phenomena in Fe(II) complexes. *Chem. Soc. Rev.*, 29:419–427, 2000.
- [3] P. M. Raccah and J. B. Goodenough. First-order localized-electron collective-electron transition in LaCoO_3 . *Phys. Rev.*, 155(3):932–943, 1967.
- [4] Kichizo Asai, Peter Gehring, Henry Chou, and Gen Shirane. Temperature-induced magnetism in LaCoO_3 . *Phys. Rev. B*, 40:10982–10985, 1989.
- [5] Kichizo Asai, Atsuro Yoneda, Osamu Yokokura, J. M. Tranquada, G. Shirane, and Key Kohn. Two spin-state transitions in LaCoO_3 . *J. Phys. Soc. Jpn.*, 67(1):290–296, 1998.
- [6] T. Vogt, J. A. Hriljac, N. C. Hyatt, and P. Woodward. Pressure-induced intermediate-to-low spin state transition in LaCoO_3 . *Phys. Rev. B*, 67(14):140401, 2003.
- [7] J. Baier, S. Jodlauk, M. Kriener, A. Reichl, C. Zobel, H. Kierspel, A. Freimuth, and T. Lorenz. Spin-state transition and metal-insulator transition in $\text{La}_{1-x}\text{Eu}_x\text{CoO}_3$. *Phys. Rev. B*, 71(1):014443, 2005.
- [8] S. Yoshida, W. Kobayashi, T. Nakano, I. Terasaki, K. Matsubayashi, Y. Uwatoko, I. Grigoraviciute, M. Karppinen, and H. Yamauchi. Chemical and physical pressure effects on the magnetic and transport properties of the a-site ordered perovskite $\text{Sr}_3\text{YCo}_4\text{O}_{10.5}$. *J. Phys. Soc. Jpn.*, 78:094711, 2009.
- [9] S. Kimura, Y. Maeda, T. Kashiwagi, H. Yamaguchi, M. Hagiwara, S. Yoshida, I. Terasaki, and K. Kindo. Field-induced spin-state transition in the perovskite cobalt oxide $\text{Sr}_{1-x}\text{Y}_x\text{CoO}_{3-\delta}$. *Phys. Rev. B*, 78(18):180403, 2008.
- [10] M. A. Korotin, S. Yu. Ezhov, I. V. Solovyev, V. I. Anisimov, D. I. Khomskii, and G. A. Sawatzky. Intermediate-spin state and properties of LaCoO_3 . *Phys. Rev. B*, 54:5309–5316, 1996.
- [11] S. Noguchi, S. Kawamata, K. Okuda, H. Nojiri, and M. Motokawa. Evidence for the excited triplet of Co^{3+} in LaCoO_3 . *Phys. Rev. B*, 66:094404, 2002.
- [12] G. Maris, Y. Ren, V. Volotchaev, C. Zobel, T. Lorenz, and T. T. M. Palstra. Evidence for orbital ordering in LaCoO_3 . *Phys. Rev. B*, 67:224423, 2003.
- [13] M. W. Haverkort, Z. Hu, J. C. Cezar, T. Burnus, H. Hartmann, M. Reuther, C. Zobel, T. Lorenz, A. Tanaka, N. B. Brookes, H. H. Hsieh, H. J. Lin, C. T. Chen, and L. H. Tjeng. Spin state transition in LaCoO_3 studied using soft x-ray absorption spectroscopy and magnetic circular dichroism. *Phys. Rev. Lett.*, 97:176405, 2006.
- [14] R. F. Klie, J. C. Zheng, Y. Zhu, M. Varela, J. Wu, and C. Leighton. Direct measurement of the low-temperature spin-state transition in LaCoO_3 . *Phys. Rev. Lett.*, 99(4):047203, 2007.
- [15] A. Podlesnyak, S. Streule, J. Mesot, M. Medarde, E. Pomjakushina, K. Conder, A. Tanaka, M. W. Haverkort, and D. I. Khomskii. Spin-state transition in LaCoO_3 : Direct neutron spectroscopic evidence of excited magnetic states. *Phys. Rev. Lett.*, 97:247208, Dec 2006.
- [16] Ichiro Terasaki, Soichiro Shibusaki, Shin Yoshida, and Wataru Kobayashi. Spin state control of the perovskite Rh/Co oxides. *Materials*, 3(2):786, 2010.
- [17] Soichiro Shibusaki, Ichiro Terasaki, Eiji Nishibori, Hiroshi Sawa, Jenni Lybeck, Hisao Yamauchi, and Maarit Karppinen. Magnetic and transport properties of the spin-state disordered oxide $\text{La}_{0.8}\text{Sr}_{0.2}\text{Co}_{1-x}\text{Rh}_x\text{O}_{3-\delta}$. *Phys. Rev. B*, 83:094405, Mar 2011.
- [18] Hironori Nakao, Tetsuya Murata, Daisuke Bizen, Youichi Murakami, Kenji Ohoyama, Kazuyoshi Yamada, Shintaro Ishiwata, Wataru Kobayashi, and Ichiro Terasaki. Orbital ordering of intermediate-spin state of Co^{3+} in $\text{Sr}_3\text{YCo}_4\text{O}_{10.5}$. *J. Phys. Soc. Jpn.*, 80(2):023711, 2011.
- [19] Noriyasu Furuta, Shinichiro Asai, Taichi Igarashi, Ryuji Okazaki, Yukio Yasui, Ichiro Terasaki, Masami Ikeda, Takahito Fujita, Masayuki Hagiwara, Kensuke Kobayashi, Reiji Kumai, Hironori Nakao, and

- Youichi Murakami. Unconventional magnetism in the layered oxide LaSrRhO_4 . *Phys. Rev. B*, 90:144402, 2014.
- [20] Shinichiro Asai, Noriyasu Furuta, Yukio Yasui, and Ichiro Terasaki. Weak ferromagnetism in $\text{LaCo}_{1-x}\text{Rh}_x\text{O}_3$: Anomalous magnetism emerging between two nonmagnetic end phases. *J. Phys. Soc. Jpn.*, 80:104705, 2011.
- [21] Shinichiro Asai, Noriyasu Furuta, Ryuji Okazaki, Yukio Yasui, and Ichiro Terasaki. Ga^{3+} substitution effects in the weak ferromagnetic oxide $\text{LaCo}_{0.8}\text{Rh}_{0.2}\text{O}_3$. *Phys. Rev. B*, 86:014421, 2012.
- [22] Shinichiro Asai, Ryuji Okazaki, Ichiro Terasaki, Yukio Yasui, Wataru Kobayashi, Akiko Nakao, Kensuke Kobayashi, Reiji Kumai, Hironori Nakao, Youichi Murakami, Naoki Igawa, Akinori Hoshikawa, Toru Ishigaki, Outi Parkkima, Maarit Karppinen, and Hisao Yamauchi. Spin state of Co^{3+} in $\text{LaCo}_{1-x}\text{Rh}_x\text{O}_3$ investigated by structural phenomena. *J. Phys. Soc. Jpn.*, 82(11):114606, 2013.
- [23] Shinichiro Asai, Ryuji Okazaki, Ichiro Terasaki, Yukio Yasui, Naoki Igawa, and Kazuhisa Kakurai. Weak ferromagnetic ordering disordered by rh^{3+} ions for $\text{LaCo}_{0.8}\text{Rh}_{0.2}\text{O}_3$. *JPS Conf. Proc.*, 3:014034, 2014. Proceedings of the International Conference on Strongly Correlated Electron Systems (SCES2013).
- [24] R. Eder. Spin-state transition in LaCoO_3 by variational cluster approximation. *Phys. Rev. B*, 81:035101, 2010. and references therein.
- [25] K. Knizek, J. Hejtmánek, M. Marysko, Z. Jirák, and J. Bursik. Stabilization of the high-spin state of Co^{3+} in $\text{LaCo}_{1-x}\text{Rh}_x\text{O}_3$. *Phys. Rev. B*, 85:134401, 2012.
- [26] H. Kimura, T. Moriwaki, S. Takahashi, H. Aoyagi, T. Matsushita, Y. Ishizawa, M. Masaki, S. Oishi, H. Ohkuma, T. Namba, M. Sakurai, S. Kimura, H. Okamura, H. Nakagawa, T. Takahashi, K. Fukui, K. Shinoda, Y. Kondoh, T. Sata, M. Okuno, M. Matsunami, R. Koyanagi, Y. Yoshimatsu, and T. Ishikawa. Infrared beamline BL43IR at SPring-8:: design and commissioning. *Nuclear Instr. Methods Phys. Res. A*, 467–468, Part 1:441–444, 2001.
- [27] S Tajima, A Masaki, S Uchida, T Matsuura, K Fueki, and S Sugai. Infrared reflectivity and electronic states in perovskite-type oxides $\text{La}_{1-x}\text{Sr}_x\text{FeO}_3$ and $\text{La}_{1-x}\text{Sr}_x\text{CoO}_3$. *J. Phys. C*, 20(23):3469, 1987.
- [28] S. Yamaguchi, Y. Okimoto, and Y. Tokura. Local lattice distortion during the spin-state transition in LaCoO_3 . *Phys. Rev. B*, 55:R8666–R8669, Apr 1997.
- [29] A. Doi, J. Fujioka, T. Fukuda, S. Tsutsui, D. Okuyama, Y. Taguchi, T. Arima, A. Q. R. Baron, and Y. Tokura. Multi-spin-state dynamics during insulator-metal crossover in LaCoO_3 . *Phys. Rev. B*, 90:081109, Aug 2014.
- [30] S. Mukhopadhyay, M. W. Finnis, and N. M. Harrison. Electronic structures and phonon free energies of LaCoO_3 using hybrid-exchange density functional theory. *Phys. Rev. B*, 87:125132, Mar 2013.